Journal of King Saud University - Science 36 (2024) 103085

HOSTED BY

Contents lists available at ScienceDirect

Journal of King Saud University - Science

journal homepage: www.sciencedirect.com

Full Length Article

Effective removal of heavy metals from aqueous solution using CS/OMMT nanocomposite synthesized by gamma irradiation

Abdullah A. Al-Kahtani

Department of Chemistry, College of Science, King Saud University, P. O. Box 2455, Riyadh 11451, Saudi Arabia

ARTICLE INFO

Keywords:
Nanocomposite
Heavy metal
Adsorption isotherm
Adsorption kinetics

ABSTRACT

The current investigation involved the fabrication of nanocomposites CS/OMMT through polymerization initiated by γ-rays irradiation. The product was characterized using FTIR and SEM techniques. The current analysis aimed to determine the adsorption performance of lead (II) ions onto nanocomposites that were synthesized, using a batch adsorption technique in an aqueous medium. The investigation analyzed the influence of different issues on the adsorption capability of the nanocomposite. Further, the lead (II) concentration, medium pH, contact time & adsorbent use were taken into account. Adsorption process order was determined with the help of kinetics. Kinetics data of pseudo 1st and 2nd order models were analyzed. There was a strong correlation between the data and the second-order kinetic model. Based on our research, we conclude that the nanocomposite showed good agreement with the Langmuir model of Pb(II) ions. The nanocomposite underwent a desorption procedure utilizing solutions of $CaCl_2$, NaCl and 0.01 M HNO_3 to attain complete elimination of Pb(II) ions. This process are revealed that CS/OMMT demonstrated remarkable efficacy as an absorbent for heavy metal ions, suggesting its potential as a viable method for purifying heavy metal-contaminated water.

1. Introduction

Heavy metal-contaminated wastewater is being dumped into natural water reservoirs in increasing quantities (Prakash et al., 2012). Heavy metals and other toxic discharges have increased as industrial activity has grown. The World Health Organisation (WHO) lists Pb, Cd, Zn, Ni, Co, Cr, Cu, and Hg as the primary heavy metals of concern. Ions of such heavy metals cause serious public health issues and may be very hazardous to aquatic life when they contaminate fresh, potable water. Pb, Ni, Cu, Hg, Cr, Cd, and as are only some of the most widely distributed heavy metals. These metals are being released by several industrial activities such as dental operations, textiles, tanning, plating and pulp industry (Sampath et al., 2014). Since current heavy metal removal technologies tend to be expensive and restricted, it's important to develop alternative methods that make use of readily accessible, low-priced materials. The adsorption technique has been confirmed to be a cost-effective and efficient for cleaning up waste waters. As an additional bonus, activated carbon is a popular adsorbent (Chen et al., 2008). Lead ions can be unsafe to humans because they react with the sulfhydryl group in proteins. In addition to restraining root increase and diminishing capillary control of plants (Mishra et al., 2013; Mahida and Patel, 2016), Pb ions are harmful to aquatic creatures. These concerns highlight the need to eliminate the heavy metal ions from their usual habitats. Currently, adsorption-based processes are considered among the most exciting approaches due to an ease of handling adsorbents, efficiency and low cost (Zhong et al., 2013). Chitosan, a biopolymer derived from chitin, is a spectacular component of many organisms. Chitosan has an intrinsic character in the process of metal extraction, making it a suitable option for the creation of polymer nanocomposite with increased performance. The chitosan compound to adsorb heavy metals and improve by addition of additives such as nanoparticles (Sampath et al., 2014).

Researchers are considering using nanocomposites as adsorbents to clean up wastewater contaminated with heavy metals (Rahbar et al., 2014). Nanotechnology is regarded as a potent substitute since adsorbents in nanotechnology exhibit a considerably high area-to-volume ratio, thereby enabling novel and effective techniques for eliminating diverse chemical contaminants, particularly in aqueous environments (Qu et al., 2013; Ferrero et al., 2014; Wang et al., 2015; Mulvaney and Chang, 1977). Jayakumar et al. (Jayakumar et al., 2013) used glutaraldehyde-chitosan/Nylon6/Polyurethane foam to remove lead II ions from water. The adsorption process showed first order kinetics and the pH. Temperature decreases metal adsorption, according to Morales-Futalan et al. They used bentonite-immobilized chitosan. (Futalan et al., 2011). Ferrero coated cotton gauze with chitosan to eliminate Cu(II) and Cr(VI) from aqueous sample. The researchers discovered that the most favorable adsorption occurred at a neutral pH of 3 for chromium (VI) and at a slightly acidic pH of 5 for copper (II) ions, as reported in reference (Ferrero et al., 2014). The study conducted by Wang et al. involved an examination of the efficacy of chitosan/multiwalled carbon

https://doi.org/10.1016/j.jksus.2023.103085
Received 13 August 2023; Received in revised form 9 November 2023; Accepted 27 December 2023
Available online 5 January 2024
1018-3647/© 2024 The Author(s). Published by Elsevier B.V. on behalf of King Saud University. This is an open access article under the CC BY-NC-ND license (http://creativecommons.org/licenses/by-nc-nd/4.0/).

nanotube mateials an eliminating lead ions from aqueous solutions (Wang et al., 2015). Current work delineate the batch adsorption process of pb (II) ions using chitosan-OMMT nanocomposites. The results obtained from this study will development of potential system design applications aimed at the purification of industrial wastewater.

2. Experimental and method

2.1. Materials

Pronova Biopolymer, Inc. (USA) supplied the chitosan (CS). We calculated that the degree of deacetylation and molecular weight to be 85% and 50,000 g/mol, respectively. Aldrich Chemical Co.) supplied the triethylamine employed in this work, and it was used in its as-received laboratory grade form. Sodium montmorillonite was the clay mineral tested. Samir Tech. Chem. Pvt. Ltd. supplied lead nitrate $Pb(NO_3)_2$ with a purity of more than 99% for use in the adsorption investigations. As received, metal salts were used.

2.2. Synthesis of reactive interposing agents for clay

In this investigation, we used Mulvancy and Chang's (Mulvaney and Chang, 1977) technique for synthesising vinyl benzyl triethyl ammonium chloride (VBTAC).

2.3. OMMT preparation

To prepare OMMT, We followed the cation exchange procedure using the previously described methods by Al-Sigeny et al (Al-Sigeny et al., 2009).

2.4. Nanocomposites of CS/OMMT synthesis

We made CS/OMMT nanocomposites by using radiation cross-linking. This method involves dissolving 0.5 g of CS into 30 mL of 1 wt% acetic acid solution. This yields a 3 wt% CS solution. The CS (5 mL) was mixed with several concentrations of nanoparticles (0% to 4% OMMT) and then dispersed using ultrasonic energy for around 30 min at room temperature. Then, after 10 min, the mixture was purged with nitrogen to get rid of the oxygen. The compound was subsequently exposed to radiation at the King Abdulaziz City for Science and Technology (KACST) in Riyadh, Saudi Arabia, using a 60 Co-ray source type GC-220 supplied by Nordion INT-INC, Ontario, Canada. The ingredients were allowed to cool and then cast onto a glass plate after the reaction was complete. After the solvent was removed, films were cast from the remaining samples (Abou Taleb et al., 2012).

2.5. Characterization

The JASCO- 4600 spectrometer was used to get the FT-IR spectra. Scanning electron microscopy (SEM) provided by JEOL, Tokyo, Japan, was used to look at the surface morphology of the copolymer.

2.6. Adsorption experiments

The wastewater was manufactured in a controlled environment. Analytical-grade $CuSO_4{\cdot}5H_2O$ was used to make the copper stock solution (0.5 M). The experiments employed recently prepared copper (II) working solutions derived from the initial solution 5 to 50 mg/L.

The technique of intake was performed in batches. For every adsorption test, the requisite adsorbent mass (0.15–0.5 g) is combined with 50 mL of copper solution. Initial pH was brought to the target range by adding hydrochloric acid (0.1 mol/L) and sodium hydroxide (0.1 mol/L) solutions, respectively. After that, you give the solution 10 min of room temperature stirring at a pace of roughly 150 revolutions per minute. The quantification of residual metal in the solution was performed by UV spectrophotometer. Three independent replicates of each experiment were conducted for each analysis. The amount of the ion Cu^{2+} removed was then calculated as:

$$Metal\ removed\ (mg/g(=C_0–C_1/W$$

where C_0, C_1 are the concentrations of Cu^{2+} ions before and after uptake, respectively.

The study involved the preparation of multiple solutions containing 50 mg/L Cu^{2+} at an adsorbent dose of 0.3 g/L. The initial pH of the solutions was varied to drop within the range of 3–8. This experimental design enabled the investigation of the power of pH on the release of Cu^{2+} ions.

2.7. Reusability and stability

Solutions of HNO_3 and NaCl was used to perform the desorption experiments, where 10 mL of 0.01 mol/L nitric acid (HNO_3) and sodium chloride (NaCl) solutions were used under 1 min sonication to desorb Pb^{2+} from 50 mL of 50 mg/L Pb(II) solution. After the extraction of the nanocomposite from the desorption medium, an assessment was conducted to determine the concentration of Pb^{2+} ions. The efficacy of the CS/OMMT's reusability was evaluated through the utilisation of a 10 mL solution of 2 mol/L NaOH, which was subjected to 1 min of sonication and washed with deionized water (Abou Taleb et al., 2012). The aggregate level of uncertainty across all experiments was determined to fall within the interval of 3–4 percentage.

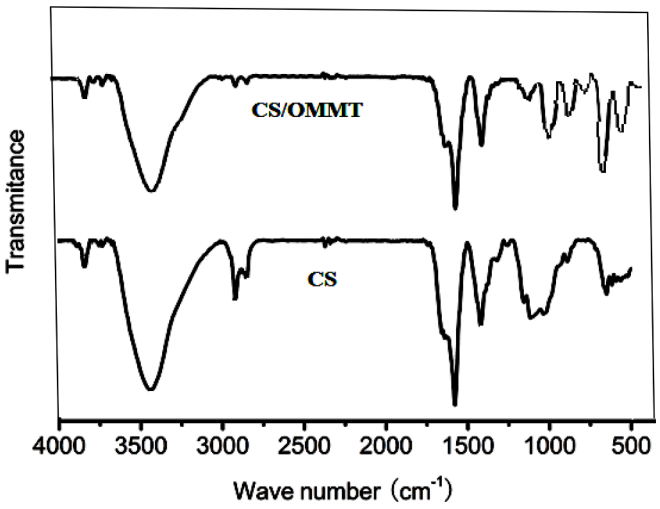

Fig. 1. FTIR spectra of CS and CS/OMMT nanocomposite.

3. Result and discussions

The samples were prepared utilizing γ-ray irradiation as a cross-linking agent and free radical initiator. The utilization of OMMT as a crosslinking agent is feasible owing to the presence of quaternary ammonium within it, particularly in the existence of C = C bonds. The reaction between OMMT and CS monomers results in the formation of a gel, as reported in (Al-Sigeny et al., 2009). The existence of the nitrogen atom was confirmed by EDX studies.

3.1. FTIR analysis

FTIR analysis of both CS and CS/OMMT nanocomposites are shown in Fig. 1. The FTIR spectra exhibits the band at approximately 3500 cm^{-1}, indicating the superimposition of the stretching frequency of N–H and O–H groups. The spectral features observed at 2930 and 2860 cm^{-1} are associated to stretching of the C–H bond present in the $–CH_2$ groups of CS. The band at 1650 cm^{-1} is attributed to the vibrational

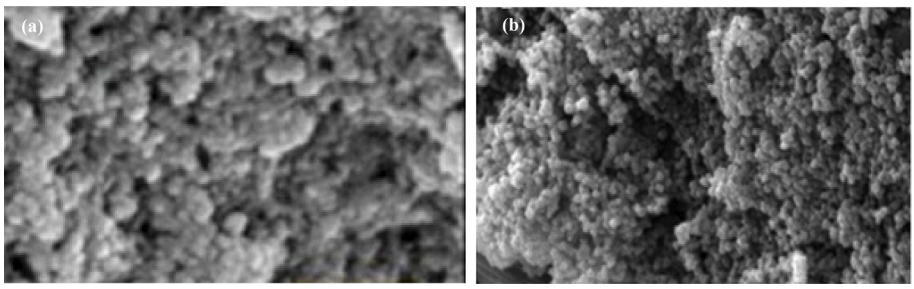

Fig. 2. SEM of the prepared nanocomposites CS/OMMT (a) before adsorption of Pb ions and (b)) after adsorption of Pb ions.

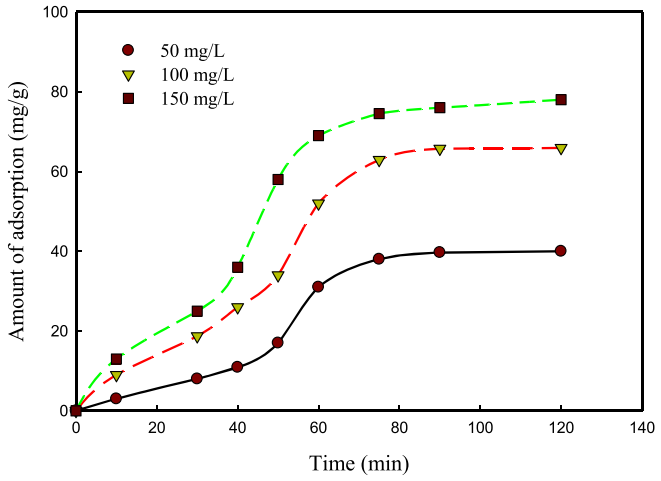

Fig. 3. Effect of contact time on adsorption capacity using CS/OMMT nanocomposite at different initial concentrations of Pb(II). The adsorbent mass was 0.5 g/L at a temperature of 25 °C and a medium pH of 5.5.

deformation of the amino (–NH_2) functional groups. The spectral feature observed at approximately 1580 cm^{-1} is associated to the N–H deformation of –NH_2 moieties. The stretching vibration of C-N is attributed to the peak observed at 1425 cm^{-1}. This outcome validates the existence of CS. The benzene ring of OMMT is identifiable by the band at 1450 cm^{-1}, as reported in reference (El-Sigeny et al., 2014). The infrared spectra obtained through Fourier-transform infrared spectroscopy (FTIR) of the CS/OMMT composite material, as depicted in Fig. 1, demonstrate the amalgamation of the absorption bands that correspond to the existence of OMMT and amine groups of chitosan. The salient spectral features to observe in nanocomposites are the –NH_2 and Si–O moieties present on the OMMT architecture. The shifted bands of –NH_2 groups at 1549 cm^{-1} and those at 1021–1080 cm^{-1} linked with Si–O groups of -MMT support the hydrogen bonding connection between NH^{3+} and the negatively charged clay sites (Oviedo Mendoza et al., 2015). Fig. 1 shows that pure CS has no C-O bond stretching vibration at 1073 cm^{-1}.

3.2. Microstructural analysis

Fig. 2a depicts the surface morphology of the CS/MMT nanocomposite, revealing a substantial layered structure with interlayer spaces. Fig. 2b depicts the minute particles present on the surface of the CS/OMMT. The Pb(II) ions can be ascribed to the small size of particles and the porous structure was observed.

3.3. Adsorption kinetics

The duration required for the remediation of metals present in water bodies is a crucial aspect from an economic standpoint. Fig. 3 shows an impact of contact time on the adsorption capacities (mg/g) of CS/OMMT

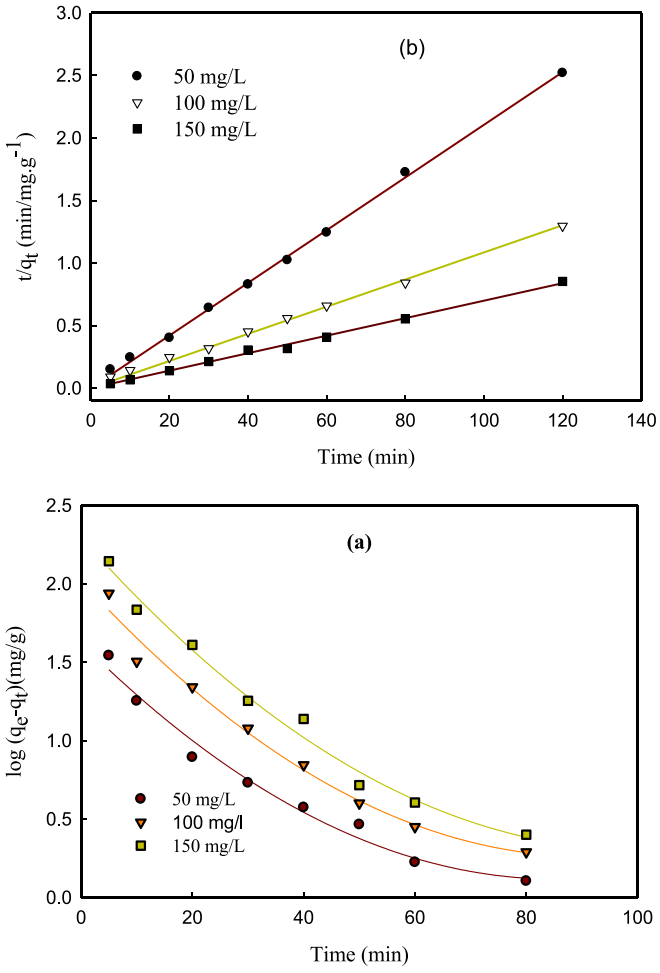

Fig. 4. (a) pseudo-first-order kinetics and (b) pseudo-second-order kinetics for the adsorption of Pb(II) ions on CS/OMMT nanocomposite.

nanocomposite at varying initial metal concentrations. The process of adsorption was observed for a duration of 120 min. Fig. 6 illustrates the kinetics of adsorption, whereby there was an initial rapid increase followed by attainment of equilibrium after 60 min. During the initial phases, there was a notable surge in rates owing to the greater availability of adsorption sites on the adsorbents. During the initial phases of the process, a significant quantity of functional groups (–OH and –NH_2) are present and can participate in complexation reactions with metal ions (Niu et al., 2017). The adsorption process experiences a deceleration over time owing to the increased diffusion range of metal into the inner surface of CS/OMMT. The gradual increase in the adsorption curve during later stages can be attributed to a slow diffusion, as stated in ref. (Azzam et al., 2016). The presence of repulsive forces renders the approach of Pb^{2+} ions towards the surface of CS/OMMT challenging.

Table 1
Pseudo-first-order and pseudo-second-order adsorption kinetic parameters of Pb (II) ions adsorption on CS/OMMT nanocomposite.

C_0 (mg L^{-1})	q_e, exp (mg g^{-1})	Pseudo-first-order			Pseudo-second-order		
		q_e, cal (mg g^{-1})	$k_1/10^{-2}$ (min^{-1})	R^2	q_e,cal (mg g^{-1})	$k_2/10^{-2}$ (g mg^{-1} min^{-1})	R^2
50	40.10	25.23	−0.798	0.922	47.9	2.965	0.998
100	65.891	61.8	−0.924	0.935	94.8	0.372	0.999
150	78.08	120.23	−01.021	0.953	142.2	1.742	0.996

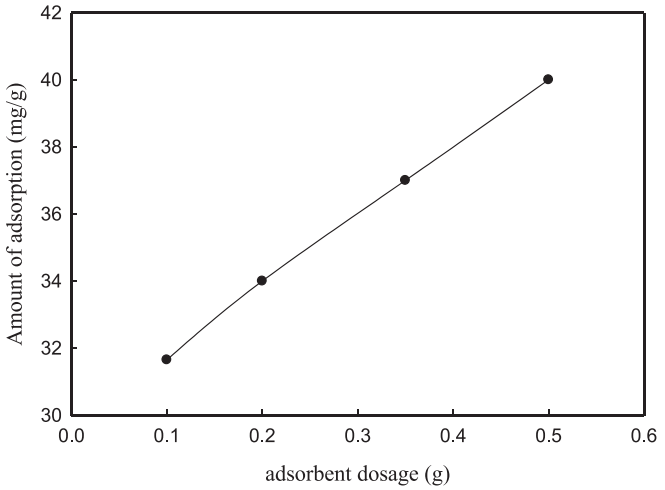

Fig. 5. Effect of adsorbent dosage on the adsorption of Pb(II) on CS/OMMT nanocomposite.

The duration of equilibrium exhibited a minor increase upon elevation in the metal ion concentration. This could be ascribed to the possibility of a greater number of Pb^{2+} ions competing for binding with CS/OMMT functional groups.

In order to clarify the adsorption characteristics of Pb^{2+} ions on CS/OMMT, the empirical data was subjected to fitting procedures utilising both pseudo 1st and 2nd order rate models. The kinetic models known as pseudo 1st and 2nd order are mathematically represented in reference (Rozaini et al., 2010; Abou Taleb et al., 2015)

$$\log(q_e - q_t) = \log q_e - \frac{k_1}{2.303}t$$

$$\frac{t}{q_t} = \frac{1}{k_2 q_e^2} + \frac{1}{q_e t}$$

Where q_e (mg/ g) represents the adsorption capacity, q_t (mg / g) is the adsorption capacity at any time t, and k_1 (min^{-1}) and k_2 (gm g^{-1} min^{-1}) are the rate constants, respectively. The kinetic parameters obtained by fitting the data using the two models, as shown in Fig. 4, are presented in Table 1. The R^2 coefficients derived from the pseudo 2nd order rate model demonstrate a strong correlation, approaching a value of one. Furthermore, the computed q_e values exhibit a high degree of concurrence with the corresponding empirical values (q_e, exp). The findings of the experiment suggest that the adsorption mechanism of Pb^{2+} ions onto CS/OMMT nanocomposites is attributed to the chemisorption process, which is consistent with the hypothesis of the 2nd order model. The deduction postulates that the covalent bond formation transpires via electron sharing between the adsorbent and metal ion, as referenced in source 22. The findings suggest that a decrease in the competition among metal ions for the binding of functional groups in nanocomposites is indicated by higher values of k_2 at lower concentrations. (Futalan et al., 2011).

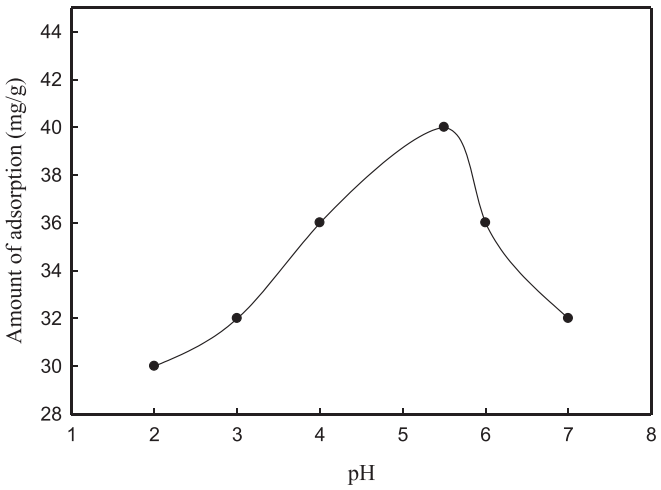

Fig. 6. Ph effect on the adsorption of pb^{2+} on CS/OMMT nanocomposite.

3.4. Effect of adsorbent dosage

Fig. 5 shows that the adsorption capacity of lead ions exhibits a gradual increase with the rise in the quantity of adsorbent from 0.1 to 0.5 g. The adsorption capacity exhibits a notable increase with a corresponding rise in the quantity of CS/OMMT adsorbent. The observed increase can potentially be ascribed to the substantial surface area of the adsorbent and the existence of functional moieties, as reported in references (Ferrero et al., 2014) and (Dinu and Dragan, 2010). Furthermore, the augmentation of active adsorption sites within the adsorbent could contribute to the expeditious escalation in the adsorption capability. The findings indicate that the various levels of adsorbent dosage are sufficient for the elimination of Pb^{2+} ions from the wastewater.

3.5. Effect of pH

The sensitivity of the adsorption capacity is observed with respect to the pH of the solution containing metal ions. The investigation of the adsorption capacities of Pb^{2+} ions on the CS/OMM nanocomposite was conducted across a range of pH values (pH = 2 to 7). Fig. 6 illustrates a gradual increase in the value of qe, ranging from 30.78 to 42.93 mg g-1, as the pH of the medium increases from 2 to 5.5. Under acidic conditions, there is an increased availability of protons that can bind to the amino groups present in chondroitin sulphate (CS). The adsorption of Pb^{2+} ions onto the nanocomposite may be reduced due to the electrostatic repulsion between Pb^{2+} and NH^{3+} ions. A decrease in q_e is observed when the pH surpasses 5.5. The precipitation of $Pb(OH)_2$ commences when the pH value surpasses 6. The examination of Pb(II) ion adsorption was not conducted beyond pH 6. The findings presented herein are consistent with prior research on the adsorption of lead onto chitosan nanocomposites (Kanchana et al., 2012). This finding additionally corroborates the chelation of metal onto the chitosan composites that were prepared, as previously reported in ref. (Azzam et al., 2016; Sheshmani et al., 2015). The findings indicate that the CS/OMMT nanocomposite possesses promising adsorption properties for the remediation of heavy metal-contaminated water sources.

3.6. Adsorption isotherm

The initial Pb^{2+} concentration was manipulated from 50 to 150 mg L^{-1} to generate adsorption isotherms to estimate CS/OMMT's maximum adsorption capability. The isotherm data was analysed utilising the Langmuir and Freundlich isotherms, both of which are widely recognised. The utilisation of Langmuir and Freundlich isotherm models is widespread in the characterization of adsorbent materials in relation to

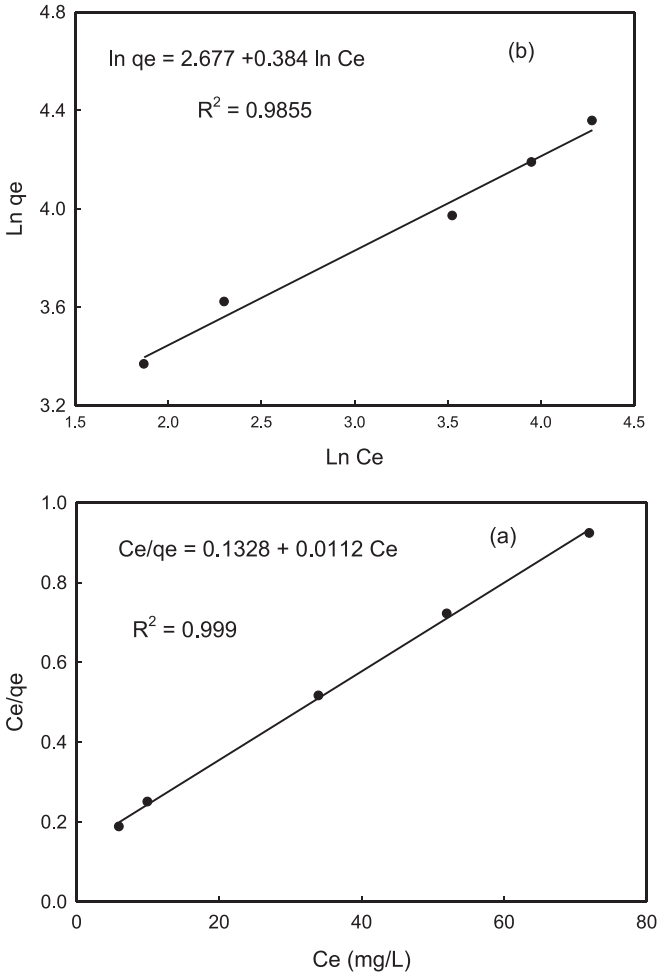

Fig. 7. Langmuir (a), and Freundlich (b) adsorption isotherms for Pb^{2+} adsorption on CS/OMMT nanocomposite.

Table 2
Langmuir, and Freundlich parameters for Pb^{2+} ions adsorption on CS/OMMT nanocomposite.

Sample	*Langmuir isotherm model*			*Freundlich isotherm model*		
	Q_{max}	K_L	R^2	1/n	k_f	R^2
CS/OMMT	89.3	0.0843	0.9990	0.384	14.54	0.9855

their adsorption properties (Niu et al., 2017). The following linear equation represents the Langmuir model:

$$\frac{C_e}{q_e} = \frac{C_e}{q_{max}} + \frac{1}{KLq_{max}}$$

Where, q_m is the Langmuir isotherm (LI) constants and K_L is the rate of adsorption, respectively. The Freundlich model is expressed as,

$$\ln q_e = \ln k_F + \frac{1}{n}\ln C_e$$

Where, K_f is the Freundlich constant and n is the heterogeneity factor, respectively. The slope and intercept of the linear plot of C_e/q_e vs. C_e (Fig. 7a) and lnqe vs. lnC_e (Fig. 7b) determine these constants. Table 2 lists all parameters. Table 2 shows that the Freundlich isotherm correlation coefficient R^2 (0.9889) is lower than Langmuir isotherm R^2 (0.999), which is confirming that it better fits for Pb^{2+} ions adsorption on CS/OMMT. Pb^{2+} ions adsorbing onto CS/OMMT formed a monolayer on a homogenous surface. Metal ions adsorb well because Pb^{2+},'s 1/n was between 0 and 1.

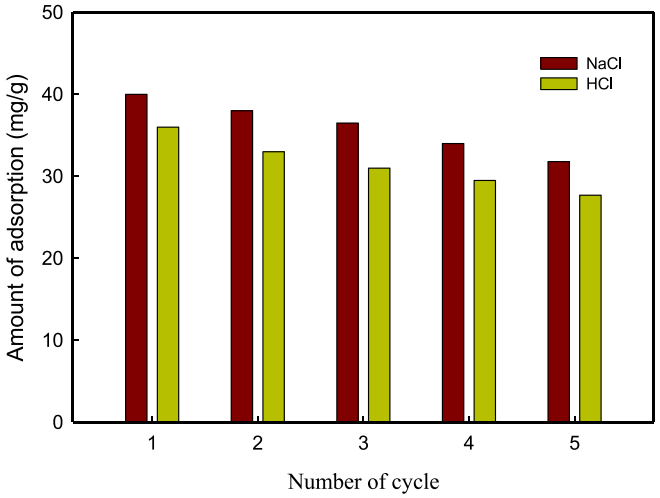

Fig. 8. Desorption and reusability studies of the adsorbent (CS/OMMT).

3.7. *Reusability and stability*

The practical application of an adsorbent is contingent upon its desorption, regeneration, and reuse performance. The desorption experiments were conducted using solutions of HNO_3 and NaCl. The CS/OMMT nanocomposite was regenerated using NaCl due to its robust chelating capability, as documented in prior studies (Niu et al., 2017; Javanbakht et al., 2016). The phenomenon of desorption observed in the NaCl solutions is ascribed to the complexation of Pb^{2+} ions. The phenomenon of desorption within the HNO_3 solution is primarily ascribed to the ion exchange process. The graphical representation in Fig. 8 demonstrates a discernible reduction in the adsorption capacity of Pb^{2+} ions after each utilization. The fields of computer science and operations and materials management technology demonstrate a high level of effectiveness in the reutilization of resources for the purpose of purifying water contaminated with Pb^{2+} ions.

4. Conclusion

The nanocomposite comprising of chitosan and OMMT has demonstrated remarkable adsorption capabilities, rendering it a favorable candidate for the elimination of Pb^{2+} ions from H_2O. The pH value of 6 was found to be the most favorable for adsorption, and the state of equilibrium was attained within a duration of two hours. The process of adsorption of Pb^{2+} ions was noticed to confirm to the pseudo 2nd kinetics, which proposes that the rate-influential step is a chemisorption stage. The adsorption isotherm of Pb^{2+} ions exhibited a good fit for LI method, suggesting that the dominant mechanism involved the formation of a monolayer on a homogeneous surface. The CS/OMMT nanocomposite exhibited the potential for multiple uses, albeit with a marginal reduction in its adsorption capacity after the 5th cycle. The findings of this inquiry suggest that the utilization of CS/OMMT is a viable option for the treatment of wastewater and the mitigation of environmental pollution.

Declaration of competing interest

The author declare that he has no known competing financial interests or personal relationships that could have appeared to influence the work reported in this paper.

Acknowledgment

The author would like to thank the Researchers Supporting Project number RSP2024R266, King Saud University, Riyad, Saudi Arabia for

their financial support.

References

Abou Taleb, M.F., Hegazy, D.E., Ismail, S.A., 2012. Radiation synthesis, characterization and dye adsorption of alginate-organophilic montmorillonite nanocomposite. Carbohydr. Polym 87 (3), 2263–2269.

Abou Taleb, M.F., El-Trass, A., El-Sigeny, S., 2015. Synthesis of polyamidoamine dendrimer (PAMAM/CuS/AA) nanocomposite and its application in the removal of Isma acid fast yellow G Dye. Polym. Adv. Technol 26, 994–1002. https://doi.org/10.1002/pat.3517.

Al-Sigeny, S., Abou Taleb, M.F., El-Kelesh, N.A., 2009. Hybrid nanocomposite prepared by graft copolymerization of 4-acryloyl morpholine onto chitosan in the presence of organophilic montmorillonite. J. Macromol. Sci. Part. A. Pure. Appl. Chem 46, 74–82. https://doi.org/10.1080/10601320802515449.

Azzam, E.M.S., Eshaq, G.h., Rabie, A.M., Bakr, A.A., Abd-Elaal, A.A., El Metwally, A.E., Tawfik, S.M., 2016. Preparation and characterization of chitosan-clay nanocomposites for the removal of Cu(II) from aqueous solution. Int. J. Biol. Macromol 89, 507–517.

Chen, A.-H., Liu, S.-C., Chen, C.-Y., Chen, C.-Y., 2008. Comparative adsorption of Cu(II), Zn(II), and Pb(II) ions in aqueous solution on the crosslinked chitosan with epichlorohydrin. J. Hazard. Mater 154, 184–191. https://doi.org/10.1016/j.jhazmat.2007.10.009.

Dinu, M.V., Dragan, E.S., 2010. Evaluation of Cu2+, Co2+ and Ni2+ ions removal from aqueous solution using a novel chitosan/clinoptilolite composite: Kinetics and isotherms. Chem. Eng. J 160, 157–163. https://doi.org/10.1016/j.cej.2010.03.029.

El-Sigeny, S., Mohamed, S.K., Abou Taleb, M.F., 2014. Radiation synthesis and characterization of styrene/acrylic acid/organophilic montmorillonite hybrid nanocomposite for sorption of dyes from aqueous solutions. Polym. Compos 35, 2353–2364. https://doi.org/10.1002/pc.22902.

Ferrero, F., Tonetti, C., Periolatto, M., 2014. Adsorption of chromate and cupric ions onto chitosan-coated cotton gauze. Carbohydr. Polym 110, 367–373. https://doi.org/10.1016/J.CARBPOL.2014.04.016.

Futalan, C.M., Kan, C.-C., Dalida, M.L., Hsien, K.-J., Pascua, C., Wan, M.-W., 2011. Comparative and competitive adsorption of copper, lead, and nickel using chitosan immobilized on bentonite. Carbohydr. Polym 83 (2), 528–536.

Javanbakht, V., Mohammad, S., Habibi, N., Javanbakht, M., 2016. A novel magnetic chitosan/ clinoptilolite/magnetite nanocomposite for highly efficient removal of Pb (II) ions from aqueous solution. Powder. Technol 302, 372–383. https://doi.org/10.1016/j.powtec.2016.08.069.

Jayakumar, S., Gomathi, T., Sudha, P.N., 2013. Sorption studies of lead (II) onto crosslinked and non-crosslinked biopolymeric blends. Int. J. Biol. Macromol 59, 165–169. https://doi.org/10.1016/J.IJBIOMAC.2013.04.031.

Kanchana, V., Gomathi, T., Geetha, V., Sudha, P.N., 2012. Adsorption analysis of Pb(II) by nanocomposites of chitosan with methylcellulose and clay. Der. Pharm. Lett 4, 1071–1079.

Mahida, V.P., Patel, M.P., 2016. Removal of heavy metal ions from aqueous solution by superabsorbent poly (NIPAAm/DAPB/AA) amphoteric nanohydrogel. Desalin. Water. Treat 57, 13733–13746. https://doi.org/10.1080/19443994.2015.1060171.

Mishra, P.C., Islam, M., Patel, R.K., 2013. Removal of Lead (II) by Chitosan from Aqueous Medium. Sep. Sci. Technol 48, 1234–1242. https://doi.org/10.1080/01496395.2012.727059.

Mulvaney, J.E., Chang, D.M., 1977. Water-soluble copolymers containing N-vinylcarbazole. J. Polym. Sci. Polym. Chem. Ed 15, 585–591. https://doi.org/10.1002/pol.1977.170150307.

Niu, Y., Li, K., Ying, D., Wang, Y., Jia, J., 2017. Novel recyclable adsorbent for the removal of copper(II) and lead(II) from aqueous solution. Bioresour. Technol 229, 63–68.

Oviedo Mendoza, M., de Fuentes, O.A., Prokhorov, E., Luna Barcenas, G., Ortega, E.P., 2015. Correlation between Electrical Properties and Potentiometric Response of CS-Clay Nanocomposite Membranes. Adv. Mater. Sci. Eng 2015, 1–6.

Prakash, N., Sudha, P.N., Renganathan, N.G., 2012. Copper and cadmium removal from synthetic industrial wastewater using chitosan and nylon 6. Environ. Sci. Pollut. Res 19, 2930–2941. https://doi.org/10.1007/s11356-012-0801-8.

Qu, X., Alvarez, P.J.J., Li, Q., 2013. Applications of nanotechnology in water and wastewater treatment. Appl. Nanotechnol. Water. Wastewater Treatment. 47 (12), 3931–3946.

Rahbar, N., Jahangiri, A., Boumi, S., Khodayar, M.J. (2014) Mercury Removal From Aqueous Solutions With Chitosan-Coated Magnetite Nanoparticles Optimized Using the Box-Behnken Design. 9:.

Rozaini, C.A., Jain, K., Oo, C.W., Tan, K.W., Tan, L.S., Azraa, A., Tong, K.S., 2010. Optimization of nickel and copper ions removal by modified mangrove barks. Int. J. Chem. Eng. Appl 84–89.

Sampath, M., Daniel, C., Sureshkumar, V., et al., 2014. Chitosan-based polymer nanocomposites for heavy metal removal. Nanocompos. Wastewater. Treat 1–22. https://doi.org/10.1201/b17789-2.

Sheshmani, S., Akhundi Nematzadeh, M., Shokrollahzadeh, S., Ashori, A., 2015. Preparation of graphene oxide/chitosan/FeOOH nanocomposite for the removal of Pb(II) from aqueous solution. Int. J. Biol. Macromol 80, 475–480. https://doi.org/10.1016/j.ijbiomac.2015.07.009.

Wang, Y., Shi, L.i., Gao, L., Wei, Q., Cui, L., Hu, L., Yan, L., Du, B., 2015. The removal of lead ions from aqueous solution by using magnetic hydroxypropyl chitosan/oxidized multiwalled carbon nanotubes composites. J. Colloid. Interface. Sci 451, 7–14.

Zhong, L., Peng, X., Song, L., Yang, D., Cao, X., Sun, R., 2013. Adsorption of Cu^{2+} and Ni^{2+} from aqueous solution by arabinoxylan hydrogel: equilibrium, kinetic, competitive adsorption. Sep. Sci. Technol 48 (17), 2659–2669.

Further reading

García-Sánchez, M.E., Pérez-Fonseca, A.A., Gómez, C., González-Reynoso, O., Vázquez-Lepe, M.O., González-Núñez, R., Manriquez-González, R., Robledo-Ortíz, J.R., 2017. Improvement of Pb(II) Adsorption Capacity by Controlled Alkali Treatment to Chitosan Supported onto Agave Fiber-HDPE Composites. Macromol. Symp 374 (1). https://doi.org/10.1002/masy.201600104.